Constrained Motions and Slow Dynamics in One-Dimensional Bosons with Double-Well Dispersion

Yang-Zhi Chou [*] and Jay D. Sau

Condensed Matter Theory Center and Joint Quantum Institute, Department of Physics, University of Maryland, College Park, Maryland 20742, USA

(Received 31 May 2023; accepted 21 December 2023; published 22 January 2024)

We demonstrate slow dynamics and constrained motion of domain walls in one-dimensional (1D) interacting bosons with double-well dispersion. In the symmetry-broken regime, the domain-wall motion is "fractonlike"—a single domain wall cannot move freely, while two nearby domain walls can move collectively. Consequently, we find an Ohmic-like linear response and a vanishing superfluid stiffness, which are atypical for a Bose condensate in a 1D translation invariant closed quantum system. Near Lifshitz quantum critical point, we obtain superfluid stiffness $\rho_s \sim T$ and sound velocity $v_s \sim T^{1/2}$, showing similar unconventional low-temperature slow dynamics to the symmetry-broken regime. Particularly, the superfluid stiffness suggests an order by disorder effect as ρ_s increases with temperature. Our results pave the way for studying fractons in ultracold atom experiments.

DOI: 10.1103/PhysRevLett.132.046001

Introduction.—Ultracold neutral atom systems have been a promising platform for studying novel quantum many-body phenomena. Particularly, the ability to control interacting bosons motivates substantial new fundamental research [1–14] that does not have solid-state analogs. For example, interacting bosons with double-well dispersion (with two dispersion minima at $k = \pm k^*$) can be realized in the experiments [6,10,12] with at least three distinct approaches. One can achieve double-well dispersion by using two counterpropagating Raman laser lights that effectively create spin-orbit coupling for the pseudospin-1/2 bosons [6,15,16]. Alternatively, a bosonic ladder with π flux per plaquette (by laser-assisted tunneling [17]) generates double-well dispersion with the chain degrees of freedom acting like the pseudospins [18–20]. Lastly, shaking an optical lattice with a frequency close to the energy difference between the ground band and the first excited band can realize double-well dispersion [10,12]. Interacting bosons with double-well dispersion allow for rich quantum phase diagrams and novel dynamical response [21–37].

Bose condensates with double-well dispersion are highly nontrivial, even without internal degrees of freedom (e.g., pseudospin). The two dispersion minima can be viewed as Z_2 degrees of freedom, and a Z_2 symmetry-breaking phase transition (analogous to an Ising ferromagnetic transition [6]) occurs at low temperatures for repulsively interacting bosons. Topological defects appear as domain walls separating regimes with different momenta. Intriguingly, the domain walls are stable and can persist for hundreds of milliseconds in the experiments [10,12], implying slow relaxation in the low-temperature (but $T \neq 0$) symmetry-broken regime.

In this work, we study the dynamics of one-dimensional (1D) interacting single-component bosons with double-well dispersion as summarized in Fig. 1. Under spontaneous Z_2 symmetry breaking, the system naturally realizes multiple domains carrying finite momenta, k^* or $-k^*$. We demonstrate that the motion of domain walls are highly constrained. A single domain wall cannot move, while two nearby domain walls can move in a collective fashion. Such intriguing kinetic properties are due to an *emergent* dipole moment conservation, which suggests a genuine connection to the "fractons" [38–57]. The constrained domain-wall motion here is in contrast to the dynamics of domain walls in the transverse field Ising model [58,59] or holons

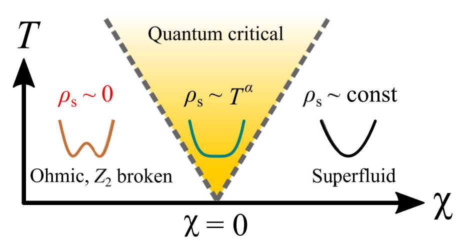

FIG. 1. Phase diagram and superfluid stiffness (ρ_s). $\chi \propto -B$ is the control parameter of the quantum phase transition. For $\chi > 0$, a dispersion with single minima is realized. ρ_s is finite and essentially temperature-independent. For $\chi < 0$, the dispersion develops two minima at $\pm k^*$, and a spontaneous Z_2 breaking takes place. ρ_s vanishes in this regime, and the corresponding transport is Ohmic-like. At $\chi = 0$, a Lifshitz dispersion (i.e., a k^4 dispersion) manifests. The renormalization group flows suggest an interacting fixed point [61,62] rather than a quantum Lifshitz Gaussian fixed point. The superfluid stiffness $\rho_s \sim T^\alpha$ with $\alpha = 1$.

and spions in 1D antiferromagnets [60]. We also develop a linear response theory for a symmetry-broken state with multiple domain walls and show vanishing superfluid stiffness and Ohmic transport, despite being a Bose condensate. Near the interacting fixed point, we develop a hydrodynamic description and find superfluid stiffness and sound velocity vanish at zero temperature, showing the incipience of slow dynamics. Remarkably, the superfluid stiffness $\rho_s \sim T$, suggesting an order by (thermal-)disorder effect. Our theory provides a natural explanation for the stable domain walls in experiments [10,12] and suggests an unprecedented way to study fractons in atomic, molecular, and optical systems.

Model.—The 1D interacting single-component bosons with a double-well dispersion are described by

$$\hat{H} = \int dx\left[-B|\partial_x b|^2 + C|\partial_x^2 b|^2 - \mu|b|^2 + \frac{U}{2}|b|^4\right], \quad (1)$$

where b is the annihilation operator for a boson, B and $C > 0$ are the coefficients controlling single-particle dispersion, μ is the chemical potential, and $U > 0$ denotes the repulsive short-range interaction. In this Letter, we focus mainly on the $B > 0$ scenario, which admits a double-well dispersion with two minima at $k = \pm k^* = \pm\sqrt{B/(2C)}$ and an energy barrier $\epsilon_0 = B^2/(4C)$ at $k = 0$. $B = 0$ is a critical point that realizes a Lifshitz dispersion (i.e., k^4). For $B < 0$, the problem is qualitatively similar to the well-known repulsive Lieb-Liniger model [63] (up to some dispersion correction).

In this work, we focus only on the superfluid phase [i.e., $U/(Bn_0) \ll 1$], where n_0 is the density. Since there are two dispersion minima ($k = \pm k^*$), it is important to determine the ground state configuration. With mean-field approximation, one can show that the ground state is the same as the "plane-wave phase" in the 1D spin-orbit-coupled BEC [16], where only one minimum is occupied. As a result, the ground state features a spontaneous Z_2 symmetry breaking, and the ground state degeneracy is 2. We adopt the standard harmonic fluid approximation in the high-density superfluid limit [64] such that the complex boson field is decomposed into the density and phase fields as follows:

$$b(x) \approx \sqrt{n_0 + \delta n(x)}e^{i\phi(x)}, \quad (2)$$

where n_0 is the density, δn encodes the local fluctuation of density, and ϕ is the phase field. Using the expression of b in Eq. (2), we can rewrite Eq. (1) with the two dynamical variables, ϕ and δn. For $|\delta n| \ll n_0$, we can integrate out δn_0 in the imaginary-time path integral and obtain a phase-only action. After rescaling of the parameters, we obtain an imaginary-time action $\mathcal{S}_{\mathrm{eff}}$ given by [65]

$$\mathcal{S}_{\mathrm{eff}} \approx \int d\tau dx\left[\frac{1}{2}(\partial_\tau\theta)^2 + \frac{1}{2}(\partial_x^2\theta)^2 + \frac{r}{2}(\partial_x\theta)^2 + u(\partial_x\theta)^4\right], \quad (3)$$

where τ is the rescaled imaginary time, θ is the rescaled phase field, $r \propto -B$, and u is the effective interaction of the phase fields. Equation (3) is strictly valid for $\delta \equiv \mu/\epsilon_0 \gg 1$. For $\delta \ll 1$, density fluctuation cannot be ignored near a domain wall [29]. We focus only on the limit $\delta \gg 1$ and $u > 0$. Since much of our analysis ultimately relies on the low energy degrees of freedom, i.e., domain walls and phonons, our conclusions are not qualitatively changed in the other limit as discussed in the Supplemental Material [65].

Constrained motion and conservation of dipole moments.—The 1D bosons with a double-well dispersion manifest spontaneous Z_2 symmetry breaking, analogous to a ferromagnetic transition. To see this, we introduce $m(x) = \partial_x\theta$, which corresponds to the momentum density of the superfluid. The static part of Eq. (3) becomes the standard Landau theory for an Ising magnet, $(r/2)m^2 + \frac{1}{2}(\partial_x m)^2 + um^4$. For $r < 0$, the $\langle m\rangle \neq 0$ features a spontaneous symmetry breaking. At zero temperature, the m is spatially uniform, and $|m| = m_0 = \sqrt{|r|/(4u)}$. At small finite temperatures, the system develops multiple domains with alternating signs of m (corresponding to the slope of θ) as illustrated in Fig. 2. The density of domain walls is proportional to $\exp(-E_{\mathrm{DW}}/T)$, where E_{DW} is the energy cost for creating one domain wall [29]. The dynamics in a state with multiple domain walls is highly unusual as we show in the following.

First, we discuss the single-domain-wall solution. An "up-pointing" single-domain-wall is described by [29]

$$\theta_{\mathrm{DW}}(x) = \theta_0 + m_0\sqrt{\frac{2}{|r|}}\ln\left[\cosh\left(\sqrt{\frac{|r|}{2}}(x - x_0)\right)\right], \quad (4)$$

where the domain-wall position is x_0. When $\sqrt{|r|}|x - x_0| \gg 1$, $\theta_{\mathrm{DW}}(x)$ recovers the slope m_0 for $x > x_0$ and $-m_0$ for $x < x_0$. Remarkably, moving a single domain wall will violate the energy constraint in Hamiltonian by forcing slopes to deviate from the equilibrium value $\pm m_0$. Thus, the motion of a single domain wall is suppressed due to the potential energy. However, one can move the entire domain while satisfying the potential energy (the blue segment in Fig. 2). As a result, two nearby domain walls can move simultaneously. The constrained domain-wall motion here is a direct consequence of momentum conservation (i.e., spatial translation invariant) of the 1D interacting bosons with double-well dispersion because moving a single domain wall will result in a change in the momentum of the condensate.

To understand the constrained domain-wall motion further, we examine the states with multiple domains more closely. First, we label the two types of domain walls to positive charge (up-pointing) and negative charge

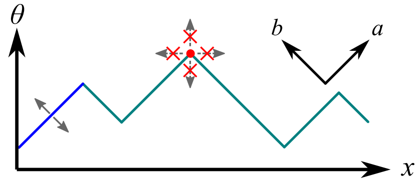

FIG. 2. Motion of domain wall in the symmetry-broken phase. In each domain, $|\partial_x\theta| = m_0$, where $m_0 = \sqrt{|r|/(4u)}$. A single domain wall (e.g., the red dot) cannot move freely because of the energy penalty, while an entire domain (e.g., the blue segment) can move. The directions of collective coordinates a and b correspond to the movement of domains. The domain-wall positions are labeled by x_n.

(down-pointing). The total dipole moment of the domain-wall charges is given by

$$\mathcal{D} = \sum_n (x_{2n} - x_{2n-1}), \tag{5}$$

where x_n indicates the position of the nth domain wall (as illustrated in Fig. 2). The alternating domains can be characterized by $\{[\theta(x_{n+1}) - \theta(x_n)]/(x_{n+1} - x_n)\} = (-1)^{n+1} m_0$ without loss of generality. Using this configuration, we can show that

$$\mathcal{D} = m_0^{-1} \sum_n [\theta(x_{2n}) - \theta(x_{2n-1})] = 2\pi Q m_0^{-1}, \tag{6}$$

where $Q = (1/2\pi)\int dx \partial_x \theta$ is related to the total momentum, which governs the boundary condition. Thus, the total dipole moment $\mathcal{D}$ is a conserved quantity associated with the boundary condition of θ. We note that the conservation of $\mathcal{D}$ (the dipole moment of topological defects) is dictated by the energy constraint, and the dipole moment conservation is an emergent low-temperature description when phonons can be ignored. The conservation of dipole moment suggests a relation to the fractons [38–45,47–57] that is known for its constrained dynamics of excitations. Our result suggests that the domain walls of 1D bosons with double-well dispersion can be viewed as fractons.

Phonon and relaxation mechanism.—In addition to domain walls, the low energy dynamics of the system contains gapless phonon degrees of freedom as well. To understand the interplay between phonons and domain walls, we consider a long-wavelength variation $\delta\theta(x)$ on top of a single domain-wall profile θ_{DW} [Eq. (4)]. We can construct a solution such that the entire $x < x_0$ domain displaces slightly (corresponding to the blue domain motion in Fig. 2) while the $x > x_0$ domain remains the same. For $|x|\sqrt{|r|/2} \gg 1$ (i.e., sufficiently away from the domain wall), we find that $\delta\theta(x \to -\infty) \neq 0$ and $\delta\theta(x \to \infty) = 0$, corresponding to a perfect reflection at the domain wall [65]. The phonons in each domain couple through the motion of the domain walls. Thus, we can integrate out the phonons in each domain wall and focus on the dynamics of the domain walls.

Integrating out the nearly perfectly reflecting phonons leads to two forces on the domain walls: a Casimir effect and phonon drag. The Casimir effect is generated by the standing waves formed by the phonons in each domain, and it tends to stabilize configurations with equally spaced domain walls. The phonon drag is a friction force that arises from the "radiation pressure" as a moving domain wall experiences imbalance fluxes of momentum on the two sides (due to the longitudinal Doppler shift). The phonon drag can be described by a force $F_{\mathrm{drag}} = -\gamma v$, where γ is the coupling constant. The phonon fluctuations responsible for the drag also lead to diffusive motion of the domains with a velocity determined by the fluctuation dissipation theorem [65]. A direct consequence of the domain diffusion is an unusually slow dynamics (as compared to other systems, e.g., the transverse-field Ising model [58,59]). See [65] for a discussion.

Ohmic response and vanishing superfluid stiffness.—To further quantify the slow dynamics of the domain walls, we study the transport properties in the symmetry-broken regime. Transport in the condensate is determined by the response to a vector potential $A \geq 0$, equivalent to tilting the optical lattice in the experiments [2,69]. The vector potential A and θ satisfy the following gauge transformation: $A \to A + \partial_x \Lambda$ and $\theta \to \theta + \Lambda$. Therefore, we can incorporate the effect of vector potential by the minimal substitution: $\partial_x\theta \to \partial_x\theta - A$. In the presence of a uniform vector potential A, the minimal momenta become $m_0 + A$ and $-m_0 + A$, indicating that A modifies the slope in each domain. Assuming $0 < A < m_0$, one can easily find new configurations that follow the change of slopes in θ without changing the boundary phase $\Delta\theta$. In addition, the ground state energy with n domain walls ($n > 1$), $E_n[\theta(x)]$ does not depend on A, suggesting an emergent rank-two gauge symmetry, $E_n[\theta(x)] = E_n[\theta(x) - Ax]$ [46]. Intuitively, such properties imply the absence of response to a finite A, indicating a state with zero superfluid stiffness despite locally being a Bose condensate. In fact, the supercurrent (i.e., distortion of slope) due to an application of a vector potential can relax by dissipating energy into the phonon drag. The result is a finite relaxation time for the current that is similar to the decay of current following a transient electric field in an Ohmic conductor.

To confirm the absence of superfluid stiffness, we develop a linear response theory for the symmetry-broken states and derive the Ohmic transport [65]. The goal is to derive the effective action of A by integrating out the domain-wall degrees of freedom. For simplicity, we assume a strong Casimir potential such that the domain walls are equally spaced and the domain size is $\bar{l}$. In the presence of A, we assume $\partial_x\theta = (-1)^{n+1} m_0 + h(x)$ for $x_n < x < x_{n+1}$, where $h(x)$ is a response to the applied vector potential A. Then, we integrate out the fluctuations at the Gaussian level and derive an effective action for A as follows:

$$\mathcal{S}_{A,\mathrm{eff}}\Big|_{k=0} \equiv \frac{\bar{l}}{\beta}\sum_{\omega_m} Q(\omega_m)\tilde{A}(-\omega_m)\tilde{A}(\omega_m).$$

The ac conductivity and superfluid stiffness can be obtained by $\sigma_{\mathrm{ac}}(\omega) \propto (i/\omega)Q(\omega_m \to -i\omega - 0^+)$ and $\rho_s \propto Q(\omega_m = 0)$. When $\gamma \neq 0$, we obtain an Ohmic response in the real part of low-frequency conductivity:

$$\mathrm{Re}[\sigma_{\mathrm{ac}}(\omega)] \propto \frac{16m_0|r|^2\gamma(8m_0^2|r| + \gamma^2)\bar{l}}{(8m_0|r|\gamma)^2 + [(8m_0^2|r| + \gamma^2)\omega\bar{l}]^2}. \quad (7)$$

Moreover, the superfluid stiffness ρ_s vanishes exactly, suggesting insulating behavior in a Bose condensate. Although the analytical results are derived with the equal-spaced domain-wall assumption, the qualitative results remain the same for general situations as apparent from the numerical results discussed later.

In addition, we study the problem using a discretized Gross-Pitaevski equation [65], which can simulate bosons in the semiclassical limit. The main goal of our simulation is to confirm the Ohmic response of the finite-temperature states with a few domain walls. To do this, we choose initial conditions $\psi_j = e^{i\theta_j}$ together with a choice for the phase variable θ_j where the sign of the slope of θ_j varies across domain walls in space. In addition, we assume that the system is subject to a large uniform electric field for a short time, which as discussed in the previous subsection, corresponds to a tilting of the phase profile $\theta_j \to \theta_j + Aj$. The ensuing dynamics obtained from the numerical solution of the Gross-Pitaevski equation, shown in Fig. 3(a), confirms the relaxation of the phase profile to a configuration where the slopes obey the ground state value as time progresses through the simulation.

To understand the observable transport consequences of this relaxation we compute the discrete local current operator. In Fig. 3(b), we show the current profiles for a few representative times corresponding to the phase profiles in Fig. 3(b). There are two important messages here. First, the current relaxes, suggesting a nonsuperfluid behavior. Second, the average current decreases substantially from the initial value, suggesting a vanishing current in the long-time limit. The decay of current confirms the Ohmic transport as predicted by our linear response theory.

In continuous 1D systems with momentum conservation, thermodynamic states can be associated with a certain momentum density. Such states, which result from the application of an electric field, carry a current even after the electric field is switched off. The resulting transport is effectively ballistic corresponding to infinite conductivity. In our case with Z_2 symmetry-broken ground states, the momentum imparted to the system can be absorbed into changing the configuration of the domain walls (see Fig. 3). Such a rearrangement transfers energy in the supercurrent into thermal energy of the phonons through a drag force on the domain walls. This dissipation of the current manifests as an Ohmic response of the current to an electric field. Our theory shows a rare example of zero superfluid stiffness and Ohmic response in a continuous translation invariant 1D system. In this case, the domain walls can be thought of as playing a similar role as the vortices in the high temperature phase of the two-dimensional superfluid where the Lorentz force on vortices from an applied supercurrent results in a dissipative voltage.

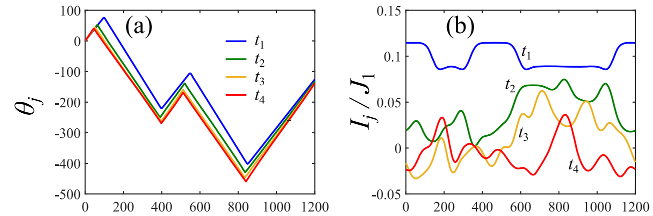

FIG. 3. Numerical results for time evolution of phase and current profiles. An initial stationary state is prepared with a vector potential $A = \pi/30$ at $t = 0$. Then, the state is evolved without a vector potential. (a) The phase configurations with different times. (b) The current configurations with different times. J_1 is the strength of the nearest-neighbor hopping in the lattice model. $t_1 = 0.0375J_1^{-1}$, $t_2 = 180J_1^{-1}$, $t_3 = 270J_1^{-1}$, and $t_4 = 360J_1^{-1}$. $L = 1200$ for all the data. See Supplemental Material for a detailed discussion of the numerical procedures.

Lifshitz quantum hydrodynamics.—The slow dynamics of the symmetry-broken phase persists all the way to the vicinity of the Lifshitz quantum critical point [11,12,30]. The quantum Lifshitz theory [i.e., Eq. (3) with $r = u = 0$] is at an unstable fixed point, and the renormalization group (RG) flows lead to an interacting fixed point with $r < 0$ and $u > 0$ [61,62]. The scaling behavior in the vicinity of a quantum critical point can be analytically derived using RG and hydrodynamic treatment [65]. The main ideas and results are summarized in the following.

First, we construct a partition function incorporating the conservation laws (i.e., particle number, energy, and momentum). Based on the partition function, we derive the finite-temperature scalings of several observable quantities using the RG results. Particularly, $\rho_M \sim T^{-1}$ corresponds to diverging inertia at zero temperature. Concomitantly, the superfluid stiffness, $\rho_s \sim T$, vanishes at zero temperature [65]. The result of stiffness shows an order by thermal disorder effect as ρ_s increases with temperature. Note that the classical gases with Lifshitz dispersion yield a different finite-temperature scaling in the inertia, $\rho_M \sim T^{-1/2}$ [65]. Another quantity of interest is the sound velocity, which can be derived using conservation laws and the thermodynamic relations. We find that the sound velocity $v_s \sim T^{1/2}$, which vanishes at zero temperature. We also note that the scaling of the Gaussian fixed point (i.e., $r = u = 0$) yields the same results as discussed in Supplemental Material [65]. The vanishing of superfluid stiffness and sound velocity at low temperatures imply that the dynamics in the quantum critical regime is very slow, qualitatively similar to the symmetry-broken regime.

Discussion.—The constrained dynamics due to the dipole moment conservation in the symmetry-broken regime indicates a connection to the fractons [38–57]. In addition, the conservation of dipole moment in our model is analogous but also distinct to the S_z conservation in several spin-$1/2$ models [70,71] that demonstrate Hilbert space fragmentation [70–79]. Both conservation laws lead to slow dynamics—however, the dipole moment $\mathcal{D}$ in this case is not microscopic but rather associated with topological defects. In contrast to systems with Hilbert space fragmentation, phonons together with slow domain motion will cause thermalization on an exponentially long timescale. This is similar to slow quantum relaxation due to dynamical constraints [80]. This long-time dynamics would include the effect of the Casimir force, which can also lead to an exponentially small in temperature residual superfluid stiffness.

The emergent dipole conservation in the symmetry-broken phase suggests that exact dipole conserving hydrodynamics [53] with vanishing superfluid stiffness and associated slow dynamics of the $u = 0$ Lifshitz critical point characterizes the critical point of our model. However, the finite $u > 0$ is a relevant perturbation that results in a different quantum critical point [61,62]. Despite this, the slow dynamics at the critical point [12] is found to survive in the form of vanishing superfluid stiffness and sound velocity. It is known that terms such as the $i\partial_\tau(\partial_x\theta)^2$ term that we ignore in our analysis can destabilize the quantum critical point in favor of a quantum fluctuation driven first order transition [81]. However, we expect our results to remain valid except very close to the quantum critical point.

Finally, we discuss the emergent symmetry in the low energy symmetry-broken regime. The ground state energy with n domain walls ($n > 1$) does not depend on the spatially uniform vector potential A, implying an emergent rank-two gauge symmetry [46]. In addition to the vanishing superfluid stiffness, the emergent symmetry may be relevant to the several interesting features discussed in this Letter. Understanding the relation between this emergent symmetry and the slow dynamics in the symmetry-broken regime is an interesting future direction.

We thank Maissam Barkeshli, Cheng Chin, Ian Spielman, Matthew Foster, Andrey Gromov, Han Pu, Chunlei Qu, Krishnendu Sengupta, and Zhi-Cheng Yang for useful discussions. This work is supported by the Laboratory for Physical Sciences, by JQI-NSF-PFC (Y.-Z. C.), by ARO W911NF2010232 (Y.-Z. C.), and by NSF DMR—1555135 (J. D. S.).

*Corresponding author: yzchou@umd.edu

[1] J. Stenger, S. Inouye, D. Stamper-Kurn, H.-J. Miesner, A. Chikkatur, and W. Ketterle, Nature (London) **396**, 345 (1998).
[2] M. Greiner, O. Mandel, T. Esslinger, T. W. Hänsch, and I. Bloch, Nature (London) **415**, 39 (2002).
[3] T. Kinoshita, T. Wenger, and D. S. Weiss, Science **305**, 1125 (2004).
[4] T. Kinoshita, T. Wenger, and D. S. Weiss, Nature (London) **440**, 900 (2006).
[5] L. Sadler, J. Higbie, S. Leslie, M. Vengalattore, and D. Stamper-Kurn, Nature (London) **443**, 312 (2006).
[6] Y.-J. Lin, K. Jiménez-García, and I. B. Spielman, Nature (London) **471**, 83 (2011).
[7] J.-Y. Zhang, S.-C. Ji, Z. Chen, L. Zhang, Z.-D. Du, B. Yan, G.-S. Pan, B. Zhao, Y.-J. Deng, H. Zhai *et al.*, Phys. Rev. Lett. **109**, 115301 (2012).
[8] J. H. Nguyen, P. Dyke, D. Luo, B. A. Malomed, and R. G. Hulet, Nat. Phys. **10**, 918 (2014).
[9] M. C. Beeler, R. A. Williams, K. Jimenez-Garcia, L. J. LeBlanc, A. R. Perry, and I. B. Spielman, Nature (London) **498**, 201 (2013).
[10] C. V. Parker, L.-C. Ha, and C. Chin, Nat. Phys. **9**, 769 (2013).
[11] K. Jiménez-García, L. J. LeBlanc, R. A. Williams, M. C. Beeler, C. Qu, M. Gong, C. Zhang, and I. B. Spielman, Phys. Rev. Lett. **114**, 125301 (2015).
[12] L. W. Clark, L. Feng, and C. Chin, Science **354**, 606 (2016).
[13] A. Putra, F. Salces-Cárcoba, Y. Yue, S. Sugawa, and I. B. Spielman, Phys. Rev. Lett. **124**, 053605 (2020).
[14] K.-X. Yao, Z. Zhang, and C. Chin, Nature (London) **602**, 68 (2022).
[15] V. Galitski and I. B. Spielman, Nature (London) **494**, 49 (2013).
[16] H. Zhai, Rep. Prog. Phys. **78**, 026001 (2015).
[17] N. Goldman, G. Juzeliūnas, P. Öhberg, and I. B. Spielman, Rep. Prog. Phys. **77**, 126401 (2014).
[18] M. Atala, M. Aidelsburger, M. Lohse, J. T. Barreiro, B. Paredes, and I. Bloch, Nat. Phys. **10**, 588 (2014).
[19] A. Celi, P. Massignan, J. Ruseckas, N. Goldman, I. B. Spielman, G. Juzeliūnas, and M. Lewenstein, Phys. Rev. Lett. **112**, 043001 (2014).
[20] A. Dhar, M. Maji, T. Mishra, R. V. Pai, S. Mukerjee, and A. Paramekanti, Phys. Rev. A **85**, 041602(R) (2012).
[21] T.-L. Ho and S. Zhang, Phys. Rev. Lett. **107**, 150403 (2011).
[22] Y. Li, L. P. Pitaevskii, and S. Stringari, Phys. Rev. Lett. **108**, 225301 (2012).
[23] H. Hu, B. Ramachandhran, H. Pu, and X.-J. Liu, Phys. Rev. Lett. **108**, 010402 (2012).
[24] W. S. Cole, S. Zhang, A. Paramekanti, and N. Trivedi, Phys. Rev. Lett. **109**, 085302 (2012).
[25] C. Qu, C. Hamner, M. Gong, C. Zhang, and P. Engels, Phys. Rev. A **88**, 021604(R) (2013).
[26] W. Zheng, B. Liu, J. Miao, C. Chin, and H. Zhai, Phys. Rev. Lett. **113**, 155303 (2014).
[27] Z. Xu, W. S. Cole, and S. Zhang, Phys. Rev. A **89**, 051604(R) (2014).
[28] M. Khamehchi, C. Qu, M. Mossman, C. Zhang, and P. Engels, Nat. Commun. **7**, 10867 (2016).

[29] T. Liu, L. W. Clark, and C. Chin, Phys. Rev. A **94**, 063646 (2016).
[30] W. S. Cole, J. Lee, K. W. Mahmud, Y. Alavirad, I. Spielman, and J. D. Sau, Sci. Rep. **9**, 7471 (2019).
[31] E. Orignac, R. Citro, M. Di Dio, and S. De Palo, Phys. Rev. B **96**, 014518 (2017).
[32] A. Tokuno and A. Georges, New J. Phys. **16**, 073005 (2014).
[33] H. C. Po, W. Chen, and Q. Zhou, Phys. Rev. A **90**, 011602(R) (2014).
[34] H. C. Po and Q. Zhou, Nat. Commun. **6**, 8012 (2015).
[35] J. Radić, S. S. Natu, and V. Galitski, Phys. Rev. A **91**, 063634 (2015).
[36] S. Sur and K. Yang, Phys. Rev. B **100**, 024519 (2019).
[37] E. Lake, T. Senthil, and A. Vishwanath, Phys. Rev. B **104**, 014517 (2021).
[38] C. Chamon, Phys. Rev. Lett. **94**, 040402 (2005).
[39] C. Castelnovo and C. Chamon, Philos. Mag. **92**, 304 (2012).
[40] J. Haah, Phys. Rev. A **83**, 042330 (2011).
[41] S. Vijay, J. Haah, and L. Fu, Phys. Rev. B **94**, 235157 (2016).
[42] M. Pretko, Phys. Rev. B **95**, 115139 (2017).
[43] M. Pretko, Phys. Rev. B **96**, 035119 (2017).
[44] A. Prem, J. Haah, and R. Nandkishore, Phys. Rev. B **95**, 155133 (2017).
[45] R. M. Nandkishore and M. Hermele, Annu. Rev. Condens. Matter Phys. **10**, 295 (2019).
[46] A. Gromov, A. Lucas, and R. M. Nandkishore, Phys. Rev. Res. **2**, 033124 (2020).
[47] M. Pretko, X. Chen, and Y. You, Int. J. Mod. Phys. A **35**, 2030003 (2020).
[48] L. Radzihovsky, Phys. Rev. Lett. **125**, 267601 (2020).
[49] A. Gromov and L. Radzihovsky, Rev. Mod. Phys. **96**, 011001 (2024).
[50] N. Seiberg, SciPost Phys. **8**, 050 (2020).
[51] S. Pai and M. Pretko, Phys. Rev. Res. **2**, 013094 (2020).
[52] E. Lake, M. Hermele, and T. Senthil, Phys. Rev. B **106**, 064511 (2022).
[53] P. Gorantla, H. T. Lam, N. Seiberg, and S.-H. Shao, Phys. Rev. B **106**, 045112 (2022).
[54] P. Gorantla, H. T. Lam, N. Seiberg, and S.-H. Shao, Phys. Rev. B **108**, 075106 (2020).
[55] P. Zechmann, E. Altman, M. Knap, and J. Feldmeier, Phys. Rev. B **107**, 195131 (2023).
[56] L. Radzihovsky, Phys. Rev. B **106**, 224510 (2022).
[57] E. Lake and T. Senthil, Phys. Rev. Lett. **131**, 043403 (2023).
[58] S. Sachdev and A. P. Young, Phys. Rev. Lett. **78**, 2220 (1997).
[59] S. Sachdev, *Quantum Phase Transitions* (Cambridge University Press, Cambridge, England, 2011).
[60] A. F. Albuquerque, C. J. Hamer, and J. Oitmaa, Phys. Rev. B **79**, 054412 (2009).
[61] K. Yang, Phys. Rev. Lett. **93**, 066401 (2004).
[62] S. Sachdev and T. Senthil, Ann. Phys. (N.Y.) **251**, 76 (1996).
[63] E. H. Lieb and W. Liniger, Phys. Rev. **130**, 1605 (1963).
[64] F. D. M. Haldane, Phys. Rev. Lett. **47**, 1840 (1981).
[65] See Supplemental Material at http://link.aps.org/supplemental/10.1103/PhysRevLett.132.046001, which includes Refs. [29,30,38,60,61,63,66–68], for derivations and extended discussions.
[66] A. Kamenev and A. Levchenko, Adv. Phys. **58**, 197 (2009).
[67] C. Hoyos, B. S. Kim, and Y. Oz, J. High Energy Phys. 11 (2013) 145.
[68] C. Hoyos, B. S. Kim, and Y. Oz, J. High Energy Phys. 10 (2014) 054.
[69] P. M. Preiss, R. Ma, M. E. Tai, A. Lukin, M. Rispoli, P. Zupancic, Y. Lahini, R. Islam, and M. Greiner, Science **347**, 1229 (2015).
[70] Z.-C. Yang, F. Liu, A. V. Gorshkov, and T. Iadecola, Phys. Rev. Lett. **124**, 207602 (2020).
[71] A. Bastianello, U. Borla, and S. Moroz, Phys. Rev. Lett. **128**, 196601 (2022).
[72] V. Khemani, M. Hermele, and R. Nandkishore, Phys. Rev. B **101**, 174204 (2020).
[73] P. Sala, T. Rakovszky, R. Verresen, M. Knap, and F. Pollmann, Phys. Rev. X **10**, 011047 (2020).
[74] T. Rakovszky, P. Sala, R. Verresen, M. Knap, and F. Pollmann, Phys. Rev. B **101**, 125126 (2020).
[75] G. De Tomasi, D. Hetterich, P. Sala, and F. Pollmann, Phys. Rev. B **100**, 214313 (2019).
[76] S. Moudgalya and O. I. Motrunich, Phys. Rev. X **12**, 011050 (2022).
[77] T. Kohlert, S. Scherg, P. Sala, F. Pollmann, B. H. Madhusudhana, I. Bloch, and M. Aidelsburger, arXiv:2106.15586.
[78] B. Mukherjee, D. Banerjee, K. Sengupta, and A. Sen, Phys. Rev. B **104**, 155117 (2021).
[79] S. Ghosh, I. Paul, and K. Sengupta, Phys. Rev. Lett. **130**, 120401 (2023).
[80] Z. Lan, M. van Horssen, S. Powell, and J. P. Garrahan, Phys. Rev. Lett. **121**, 040603 (2018).
[81] V. Kozii, J. Ruhman, L. Fu, and L. Radzihovsky, Phys. Rev. B **96**, 094419 (2017).